

CRUSTAL STRATIGRAPHY AND LIGHT TERRAIN FORMATION ON GANYMEDE: IMPLICATIONS OF RAY AND HALO IMPACT CRATERS. N. R. Baby¹, T. Kenkmann¹, K. Stephan², R. Wagner² and E. Hauber², ¹University of Freiburg, Freiburg, Germany (namitha.baby@geologie.uni-freiburg.de), ²German Aerospace Center (DLR), Institute of Planetary Research, Berlin, Germany

Introduction: Ganymede, Jupiter's largest moon, offers diverse impact crater morphologies and their ejecta blankets, which often appear as rays or halos on its icy surface. These ejecta blankets consist of bright or dark ice and non-ice materials [1, 2]. They provide insights into the subsurface composition of the terrains in which these craters are found. The light and dark terrains are formed through tectonic resurfacing and various surface processes [3]. Thus, studying these impact craters and their ejecta blankets helps us understand the vertical stratigraphy of Ganymede's crust and the tectonic processes responsible for the formation of light terrains. This study contributes to the scientific goals of the current JUICE mission to the Galilean moons.

The study is based on ballistic ejecta emplacement models [4, 5, 6] and applies these principles of excavation dynamics to gain insights into Ganymede's crustal structure.

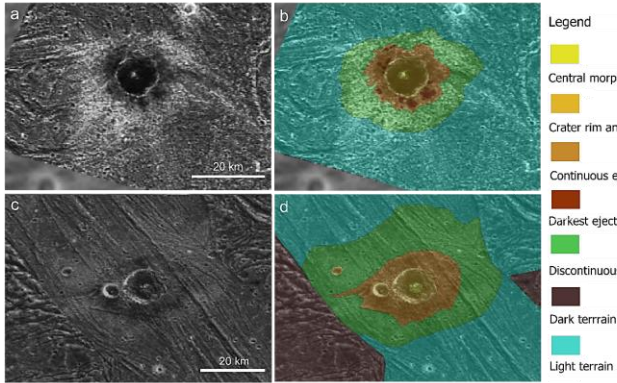


Figure 1: (a) Galileo image and (b) geologic map of DHC Khensu, (c) Galileo image and (d) geologic map of DHC Nergal

Data and Methodology: We conducted a detailed study of dark halo craters (DHCs), characterized by circular to subcircular dark ejecta surrounding the crater rim, and bright ray craters (BRCs), which feature bright ray ejecta. Morphological details of craters, including inner features and the extent of halos or rays, were mapped. Galileo NIMS data, with spatial resolutions up to ~ 2 km/pxl [1, 7], were analyzed for available craters. Using the approach in [8], we mapped the band depth (BD) of the major water ice

absorption at 1.5 or 2 μm to infer the relative abundance of water ice versus dark material.

To calculate excavation depths, we use equations from [4] and [5]

$$D_e = (1/2 D_t)(Z - 2)(Z - 1)^{(1-Z)(Z-2)} \quad (\text{Eq. 1})$$

$$D_e \approx 1/10 * D_t \quad (\text{Eq. 2}),$$

where D_e is the maximum depth of excavation,

D_t is the diameter of the transient crater cavity

Z is the Maxwell Z-model parameter

To determine the transient diameter (D_t) we use the equation from [9].

$$D = D_t^\varepsilon \cdot D_c^{1-\varepsilon} \quad (\text{Eq. 3}),$$

$D_c = 2.5$ km for Ganymede, $\varepsilon \sim 1.13$, which accounts for crater slumping [10].

$Z = 4$ streamlines are more preferred as the excavation flow in icy targets produces steeper ejection trajectories [10].

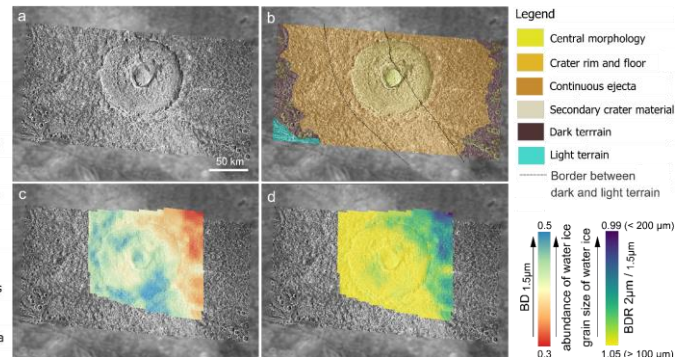


Figure 2: BRC Melkart: (a) Voyager + Galileo mosaic, (b) geologic map, (c) NIMS derived band depth map of the water ice absorption at 1.5 μm indicating the relative abundance of water ice/non-ice material and (f) grain size of water ice as derived by the NIMS derived band depth ratio map of the water ice absorptions at 2 and 1.5 μm after [8].

Results:

1. DHCs: Khensu, a ~ 17 km diameter DHC on the leading hemisphere's light terrain, has a maximum excavation depth of ~ 2.5 km (Fig. 1). Similarly, Nergal, a ~ 9 km diameter DHC on the trailing hemisphere's light terrain, has a maximum excavation depth of ~ 1.5 km (Fig. 1). Key features of DHCs include a bright peak, dark crater floor, inner dark continuous ejecta, and outer bright continuous ejecta.

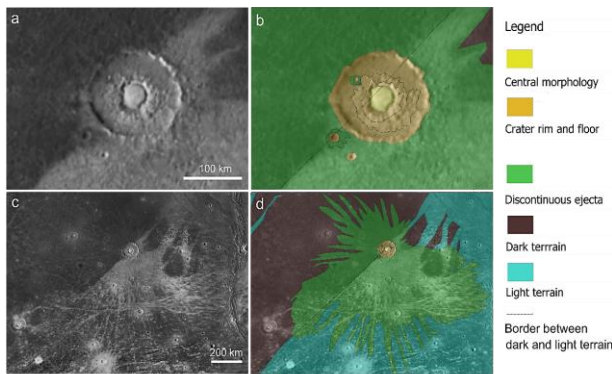


Figure 3: BRC Enkidu: (a, c) Voyager image and (b, d) detailed geologic map of Enkidu

2. BRCs: The 103 km diameter BRC, Melkart, lies at the boundary of older dark terrain and younger light grooved terrain, with a maximum excavation depth of ~12.9 km (Fig. 2 a and b). NIMS data indicate darker, less icy material concentrated along its inner crater rim, with slightly larger ice grains linked to warmer, darker regions (Fig. 2 c and d). Enkidu, a 122 km diameter crater, reaches a maximum excavation depth of ~15 km (Fig. 3). Both craters predominantly feature bright material on their floors and in their ejecta blankets.

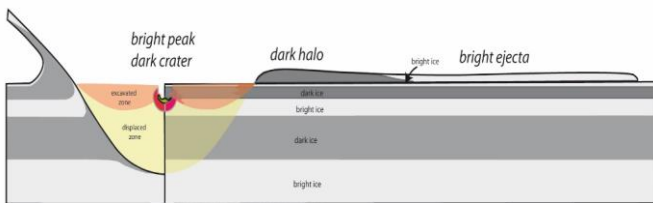


Figure 4: Schematic illustration of the subsurface layers required to explain the ejecta pattern of DHCs. In the left part is the transient cavity illustrated and how the different layers are involved in the ejecta curtain. The larger right side shows the ejecta blanket and the position of different ice layers of the target prior to impact.

Discussion: We applied Maxwell's Z-model [4] to reconstruct the subsurface's vertical stratigraphy. Regions with DHCs, such as Khensu and Nergal, exhibit alternating subsurface layers of bright and dark ice, with a thin top light terrain. The dark ejecta and crater floors of DHCs likely originate from the second and fourth layers, while the bright outer ejecta and peaks derive from the third and fifth layers (Fig. 4). In contrast, large BRCs excavate deeper into the icy crust without significant variation in ejecta brightness, indicating a simpler crustal structure dominated by bright ice. For BRCs, the exclusively bright rays imply in these regions light terrain formed via tectonic spreading (Fig. 5a). While, the presence of dark terrain

material beneath DHCs suggests that, in these regions light terrain may have formed through tectonic rifting, where dark terrain subsided into the subsurface (Fig. 5b).

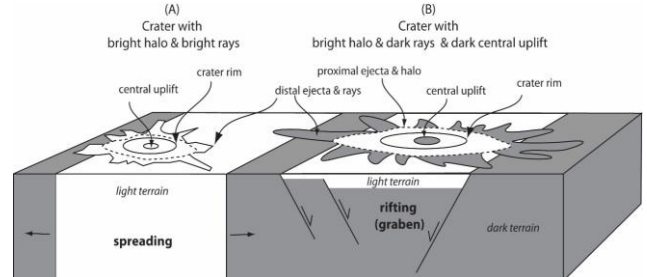


Figure 5: The ejecta facies of impact craters may help distinguish light terrains formed by tectonic spreading or rifting. BRCs are expected to form if the light terrain is formed by spreading mode of tectonism (a), while DHCs are expected when light terrain is formed by rifting mode of tectonism (b).

Acknowledgments: This project is financed by the German Aerospace Center (DLR), funding code 50QJ2403.

References: [1] Hibbitts C. A. (2023) *Icarus*, 394, 115400. [2] Schenk P. M. and McKinnon W. B. (1991) *Icarus*, 89, 318–346. [3] Pappalardo, R. T. et al. (2004) *Jupiter: The planet, satellites and magnetosphere*, 363–396. Cambridge University Press. [4] Maxwell, D. E. (1977) *Impact and explosion cratering*, 1003–1008. Pergamon Press. [5] Melosh, H. J. (1989) *Impact cratering: A geologic process*, 245. Clarendon Press. [6] Oberbeck, V. R. (1977) *Impact and explosion cratering*, 45–65. Pergamon Press. [7] Stephan, K., et al. (2008) *ScSSI*, abstr. 9060. [8] Stephan, K. et al. (2020) *Icarus*, v. 337, 113440. [9] Schenk, P. M. et al. (2004) *Jupiter: The planet, satellites and magnetosphere*, 363–396. Cambridge University Press. [10] Senft, L. E. and Stewart, S. T. (2008) *Meteoritics & Planet. Sci.*, 43, 1993–2013.